RSC Advances

PAPER

View Article Online
View Journal | View Issue

Cite this: *RSC Adv.*, 2024, **14**, 14041

Carboxyl-functionalized two-dimensional MXene–Au nanocomposites were prepared as SERS substrates for the detection of melamine in dairy products†

Dongbo Xi, [ab] Ruipeng Chen,[b] Shuyue Ren, [*b] Zhenhong Jia*[a] and Zhixian Gao*[b]

In the present study, we address the limitations of conventional surface-enhanced Raman scattering (SERS) techniques for sensitive and stable detection of melamine in food products, especially dairy. To overcome these challenges, we developed a novel SERS-active substrate by incorporating gold nanoparticles (AuNPs) onto carboxyl-functionalized two-dimensional (2D) MXene material doped with nitrides, specifically Au–Ti_2N–COOH. Our strategy leverages the unique physicochemical properties of MXene, a class of atomically thin, 2D transition metal carbides/nitrides, with tunable surface functionalities. By modifying the MXene surface with AuNPs and introducing carboxyl groups (–COOH), we successfully enhanced the interaction between the substrate and melamine molecules. The carboxyl groups form hydrogen bonds with the amino groups on the melamine's triazine ring, facilitating the adsorption of melamine molecules within the 'hotspot' regions responsible for SERS signal amplification. A series of characterization methods were used to confirm the successful synthesis of Au–Ti_2N–COOH composites.Using Au–Ti_2N–COOH as the SERS substrate, we detected melamine in spiked dairy product samples with significantly enhanced sensitivity and stability compared to nitride-doped MXene alone. The detection limit in liquid milk stands at 3.7008 μg kg^{-1}, with spike recovery rates ranging from 99.84% to 107.55% and an approximate RSD of 5%. This work demonstrates the effectiveness of our approach in designing a label-free, rapid, and robust SERS platform for the accurate quantitation of melamine contamination in food, thereby mitigating health risks associated with melamine adulteration.

Received 24th March 2024
Accepted 19th April 2024

DOI: 10.1039/d4ra02249a

rsc.li/rsc-advances

1. Introduction

Melamine, also known as cyanuramide, is a small organic molecule that contains a triazine ring. It serves as a crucial chemical raw material, with melamine–formaldehyde resin being derived from melamine as its primary constituent. Illegally adding melamine to dairy products, owing to its elevated nitrogen content, has been a concern. Ingesting excessive quantities of melamine can result in urinary calculi, crystalline urine, and acute renal failure, particularly in individuals of smaller stature, those exposed to high doses, or those with limited fluid intake.[1] Upon ingestion, melamine can react with certain intermediate degradation products to form insoluble melamine cyanuric acid salt crystals, which are highly harmful to our kidneys and can even be fatal to infants.[2] United States Food and Drug Administration (FDA) suggests setting.

A safety exposure limit for melamine and its structural analogues of less than 0.63 mg per kg bw per day. The European Food Safety Authority recommends a daily intake of 0.5 mg per kg bw per day of melamine.[3] Furthermore, the World Health Organization has set the maximum allowable content of melamine in infant formula at 1 μg g^{-1}, while the maximum allowable content for all other foods is 2.5 μg g^{-1}.[4]

To determine the protein content in milk, a milk analysis is required. The classical method for analyzing the protein content in milk is the Kjeldahl method.[5] This method is straightforward to execute and yields highly accurate results. However, it exclusively quantifies the nitrogen content in mixtures, with protein content being derived from nitrogen content calculations rather than direct measurement. Due to the high nitrogen content of melamine and its resemblance to the appearance of powdered milk, it has been illegally added to dairy products. Traditional detection methods cannot differentiate whether the nitrogen contribution arises from protein. Consequently, researchers have explored and implemented several melamine detection methods, including: High

[a]*School of Information Science and Engineering, Xinjiang University, Urumqi 830000, China. E-mail: jzhh@xju.edu.cn*

[b]*Tianjin Key Laboratory of Risk Assessment and Control Technology for Environment and Food Safety, Tianjin Institute of Environmental and Operational Medicine, Tianjin, 300050, China. E-mail: renshuyue2018@163.com; gaozhx@163.com*

† Electronic supplementary information (ESI) available. See DOI: https://doi.org/10.1039/d4ra02249a

Performance Liquid Chromatography (HPLC),[6–8] Electrochemical Analysis (ECA),[9] Infrared (IR),[10] Gas Chromatography-Mass Spectrometry (GC/MS),[11,12] Colorimetric Sensing,[13,14] ELISA[15] and Fluorescence Detection.[16,17] However, these methods have long detection times and complex preprocessing processes, requiring specialized operators. Therefore, the main objective of this study is to develop a more sensitive, convenient, and cost-effective melamine detection method. Surface-Enhanced Raman scattering (SERS) spectroscopy technique is extensively applied in fields, encompassing chemistry, biosensing, environmental science, food safety, and clinical diagnosis. Due to its remarkable attributes, including high resolution, rapidity, fingerprinting capability, real-time analysis, and non-invasive nature, SERS stands as a prominent technique for qualitative and quantitative analysis of target analytes.[18–22] Consequently, we leverage SERS to achieve swift and highly sensitive detection of the target substance. Despite the many advantages of SERS technology, such as high sensitivity and rapid detection, its relatively weak signal has been criticized. Researchers have thus employed various strategies to prepare novel SERS substrates to enhance their signal performance.

Two-dimensional (2D) materials possess advantages such as surface flatness and a large specific surface area.[23] Graphene was the first 2D material that demonstrated enhancement of the Raman signal. Since then, several 2D materials have been applied up to date. 2D materials such as transition metal dichalcogenides (TMDs) and black phosphorus (BP), hexagonal boron nitride (h-BN), have been used as SERS substrates. However, the sensitivity of these materials is generally insufficient. In 2011, Naguib and colleagues[24] have discovered a new series of 2D materials called "MXenes." These materials are generated by selectively etching the A elements from the corresponding three-dimensional (3D) MAX phases using appropriate etchants. MAX phases comprise layered ternary compounds consisting of metallic carbides, nitrides, or carbonitrides, with the general formula $M_{n+1}AX_nTx$, where M represents an early transition metal, a comprises elements from Group 13 and 14 (mainly), and X denotes carbon and/or nitrogen.[25] Tx represents surface functional groups (–O, –OH and –F).[26] As emerging 2D material MXenes have demonstrated exceptional SERS (Surface-Enhanced Raman Spectroscopy) activity. For example, He *et al.*,[27] designed a TiVC (MXene) material as a substrate with rhodamine as the Raman reporter molecule, achieving a SERS enhancement factor of 10^{12} M and a detection limit in the femtomolar range. Liu *et al.*[28] prepared a tungsten nitride ($WN\backslash W_2N\backslash W_3N_4\backslash W_2N_3$) MXene material as a substrate, with a minimum detection limit of 10^{-12} M. The SERS enhancement factor is 6.5×10^8 M. Sarycheva *et al.*[29] synthesized a Ti_2C_3 MXene material as a SERS substrate, which exhibited extensive multifunctionality. The substrate demonstrated the ability to detect various organic dyes such as methylene blue (MB), rhodamine (R6G), brilliant green (BG), malachite green (MG), crystal violet (CV), Nile Blue (NB), as well as certain harmful substances, including 1,10-phenanthroline monohydrate (PHEN), *p*-aminobenzoic acid (PABA), and 4-mercaptobenzoic acid (4-MBA), at extremely low concentrations. Peng *et al.*[30] designed Nb_2C and Ta_2C MXene substrates capable of detecting the SARS-CoV-2 spike protein at detection limits as low as 5×10^{-9} M. Lan *et al.*,[31] developed two MXene materials, vanadium carbide (V_4C_3 and V_2C), as substrates. exhibiting high SERS sensitivity, enabling rapid molecular enrichment (within 2 minutes) and achieving a molecular removal efficiency of over 95%. Additionally, this study marks the first preparation of M_4X_3-type MXene materials as SERS substrates. MXene possesses advantages such as tunable structure, topology, morphology, and surface chemistry. Beyond its application in SERS, it has found utility in photoluminescence, colorimetric sensing, electrochemistry, photothermal bioapplications, and surface plasmon resonance (SPR).[32] To further enhance the Raman signal amplification capability of the substrate, we modified the surface of Ti_2N with Au NPs (gold nanoparticles) and employed the Raman probe molecule 4-MBA (4-mercaptobenzoic acid) as a novel substrate.

This work proposes an innovative substrate utilizing Au nanoparticles (NPS) modified with carboxyl-functionalized MXene material Ti_2N, we enhance its signal amplification by introducing carboxyl groups through modification with 4-mercaptobenzoic acid (4-MBA), facilitating the detection of low concentrations of melamine in milk. The method achieves an impressively low detection limit for melamine at just 3.7008 μg kg^{-1}, requiring only straightforward pretreatment steps. This method is of significant importance for ensuring quality control and supervision in the dairy industry.

2. Materials and methods

2.1. Chemicals and reagents

Ti_2AlN (99.8%) was purchased from Jiangsu Xianfeng Nano-Technology Co., Ltd, located in Jiangsu Province, China. Chloroauric acid ($HAuCl_4$) was purchased from TaKaRa (Shanghai, China). Potassium fluoride (KF), hydrochloric acid (HCl, 35–38%), deionized water, dimethyl sulfoxide (DMSO), sodium borohydride ($NaBH_4$), chloroacetic acid (CH_2COOH), 4-mercaptobenzoic acid (4-MBA, 99.8%), cyanuric acid (99.8%), isopropanol (99.8%) were purchased from Aladdin. Melamine monoamide (99.7%), diamide cyanate (99.7%), dicyanamide (99.7%), and cypromazine (99.7%) were purchased from Macklin.

2.2. Analytical techniques

Zeta potential is analyzed at a 90° angle using the Zetasizer Nano ZS 90 instrument (Malvern Instruments Ltd, UK). The maximum range for the zeta potential is from −150 mV to 150 mV.

XPS measurements were performed on the ESCALAB 250 Xi instrument, with a binding energy scanning range of 0–1350 eV and a 1 eV per step scanning step size.

The morphological features of Ti_2N material and Au–Ti_2N–COOH material were observed using a scanning electron microscope (SEM) (Carl Zeiss Co Ltd, Germany) and a transmission electron microscope (TEM) Talos F200X (Thermo Fisher, USA).

The chemical bonding and characteristic peaks of functional groups in the Ti_2N–COOH material were measured using IS5 (Thermo Fisher, USA).

The SERS characteristic peaks of the target substance were measured using a confocal Raman laser, *via* Basis 116W21 (Renishaw, UK).

2.3. Synthesis of Au–Ti_2N–COOH

Following with the previously reported process,[25] the synthesis of Ti_2N–COOH employs a similar method. To prepare the KF–HCl mixture, dissolve 6 g of potassium fluoride (KF) in 100 mL of 6 M hydrochloric acid (HCl). Subsequently, immerse approximately 2 g of Ti_2AlN in 20 mL of the KF–HCl mixture and heat it for 3 hours. Afterward, subject the suspension to ultrasonication in a water bath at 40 °C for one hour. Following the ultrasonication step, remove the supernatant and add deionized water to the powdered material. Centrifuge the mixture at 3500 rpm for 5 minutes to eliminate soluble fluorides. Repeat the above procedure until the pH of the supernatant approaches After decanting, add isopropanol to the powder and centrifuge the mixture at 3500 rpm for half an hour. Filter the mixture to obtain ML-Ti_2NTx. Immerse 1 g of powder in 20 mL DMSO and sonicate for one hour to achieve stratification. Allow the mixture to stand overnight. Remove the supernatant, add deionized water, and centrifuge the mixture at 3500 rpm for one hour. Vacuum filter the supernatant suspension and dry it to collect FL-Ti_2NTx.

To prepare a Ti_2N–COOH solution, initiate with a Ti_2NTx solution having a concentration of 1 mg mL^{-1}. Under nitrogen gas and ice-water bath conditions, add chloroacetic acid and stir for 4 hours to prepare a Ti_2N–COOH solution. Subsequently, store the prepared colloidal solution at 4 °C for future use in the next step.

Next, utilize the prepared Ti_2N–COOH solution. Again, maintain the process under ice-water bath conditions. Introduce a 10% by-weight solution of chloroauric acid and stir for 1 hour. Gradually incorporate an excess amount of sodium borohydride ($NaBH_4$) solution. Afterward, perform centrifugation at 3500 rpm and wash the precipitate three times. Under nitrogen gas protection, subject the mixture to sonication for half an hour, creating an Au–Ti_2N–COOH solution. Store the prepared colloidal solution at 4 °C for future use in the subsequent step.

2.4. SERS spectra acquisition in milk

Ordinary brand milk purchased from a local supermarket served as the study. 10 mg of melamine was placed in a 10 mL centrifuge tube and dissolved in ultrapure water to prepare a melamine solution. The prepared melamine solution was then diluted sequentially to prepare different concentrations of melamine standard solutions, and three samples of each concentration were spiked into milk samples for testing. In the detection process, a small amount of 4-MBA solution was added to the base solution and mixed for 1 hour. Following this, the sample solution was combined proportionally with the base solution containing 4-MBA and mixed for 10 minutes. The resulting mixture solution was dropped onto a silicon wafer substrate and dried at 60 °C under vacuum, and SERS signals were detected.

3. Results and discussion

3.1. Scheme

First, synthesize the Ti_2N material. As shown in Fig. 1, chloroacetic acid was added to the successfully synthesized Ti_2N material, and the carboxyl functional group was modified on the surface of the material. Next, use chloroauric acid as the gold nanoparticle source and sodium borohydride as the reducing agent. Utilizing the material modified with carboxyl functional groups as the substrate, synthesize Au–Ti_2N–COOH material through *in situ* growth method by decorating gold nanoparticles onto the substrate. Subsequently, the detection of the target substance is achieved through Raman spectroscopy.

The carboxyl modification performed on the two-dimensional (2D) substrate composed of MXene material serves several key purposes in enhancing the performance of the SERS (Surface Enhanced Raman Scattering) substrate for the detection of melamine. The addition of gold (Au) to the carboxyl-modified MXene, specifically forming Au–Ti_2N–COOH, introduces complementary functionalities and synergistic effects that together address the challenges of sensitivity and stability in melamine detection. Here is a detailed explanation of the rationale behind this approach:

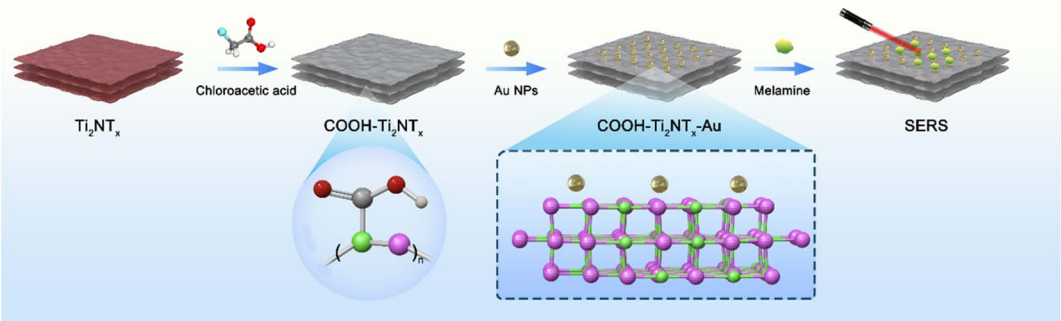

Fig. 1 Scheme of melamine SERS detection.

3.1.1. Carboxyl group-mediated target enrichment. The carboxyl groups (–COOH) introduced on the MXene surface form hydrogen bonds with the three amino groups ($-NH_2$) present on the melamine triazine ring. This specific interaction facilitates the selective and efficient capture of melamine molecules, effectively concentrating them within the vicinity of the Au nanoparticles. This targeted enrichment mechanism ensures that melamine molecules are more likely to occupy the high-field hotspots, further improving the SERS sensitivity. A plain gold film without such functionalization would lack this targeted enrichment capacity, potentially leading to reduced detection efficiency for melamine.

3.1.2. Stability and Reproducibility. The combination of MXene and Au nanoparticles in a single substrate offers enhanced stability compared to a standalone gold film. The MXene layers provide mechanical support and prevent Au nanoparticle aggregation, maintaining the substrate's structural integrity and ensuring consistent SERS performance over time. Moreover, the carboxyl groups may contribute to the stability of the Au nanoparticles by anchoring them to the MXene surface, preventing their detachment or migration during use or storage. A gold film alone might be more prone to degradation or surface oxidation, compromising the long-term reliability of the SERS substrate.

3.2. Characterization

The morphology of the Ti_2N material is being described in detail through TEM testing. As shown in Fig. 2(a), the material exhibits the characteristic layered structure of MXene materials. Fig. 2(b) presents the SEM characterization of the Ti_2N material, which confirms the layered structure of Ti_2N. Additionally, Fig. (S1) and (S2)† are SEM images taken at a relatively lower magnification, providing an overview of the Ti_2N material. In these images, the layered structure can be observed, further confirming the successful synthesis of the Ti_2N material.

Fig. 2(c) shows the infrared characterization of the synthesized Ti_2N–COOH material. For carboxyl groups (dimer) involved in hydrogen bonding, the O–H stretching vibration absorption peak appears as a broad and diffuse band in the range of 2500–3300 cm^{-1}. The carboxylic acid exhibits absorption peaks around 1400–1428 cm^{-1} and 1250 cm^{-1}, which correspond to in-plane bending vibrations of the O–H group and coupled stretching vibrations of the C–O bond. The peak observed near 920 cm^{-1} indicates the out-of-plane wagging vibrations of the O–H group. This confirms the successful modification of the carboxyl functional groups.

Fig. 2(d) shows the TEM image of the Au–Ti_2N–COOH material. According to the comparison of the scales in the figure, the particle size of gold nanoparticles is roughly in the range of 10–16 nm, and the gold nanoparticles have a slight agglomeration phenomenon, and the overall distribution is relatively uniform. A large proportion of gold nanoparticles are spaced within 10 nm to provide sufficient "hot spot" areas. Moreover, the Ti_2N material itself has a high electron density distribution of N atoms due to the transfer of electrons from Ti atoms, thus providing SERS signal enhancement ability. Therefore, the material itself has a good SERS signal amplification ability, and the gold nanoparticles are modified on its surface to further enhance the signal amplification ability of the composite. Fig. 2(e) presents the AFM characterization of the material, and in combination with Fig. (S3),† we measure the thickness of the material at 10 points from the material, through the calculation and analysis of the measured results, it can be seen that the average thickness of the material is 47.34 nm, and the RSD is about 7.27%. Fig. (S4), (S5) and Table (S1)† depict the EDS characterization of the Ti_2AlN material. From these figures, compared with the subsequent

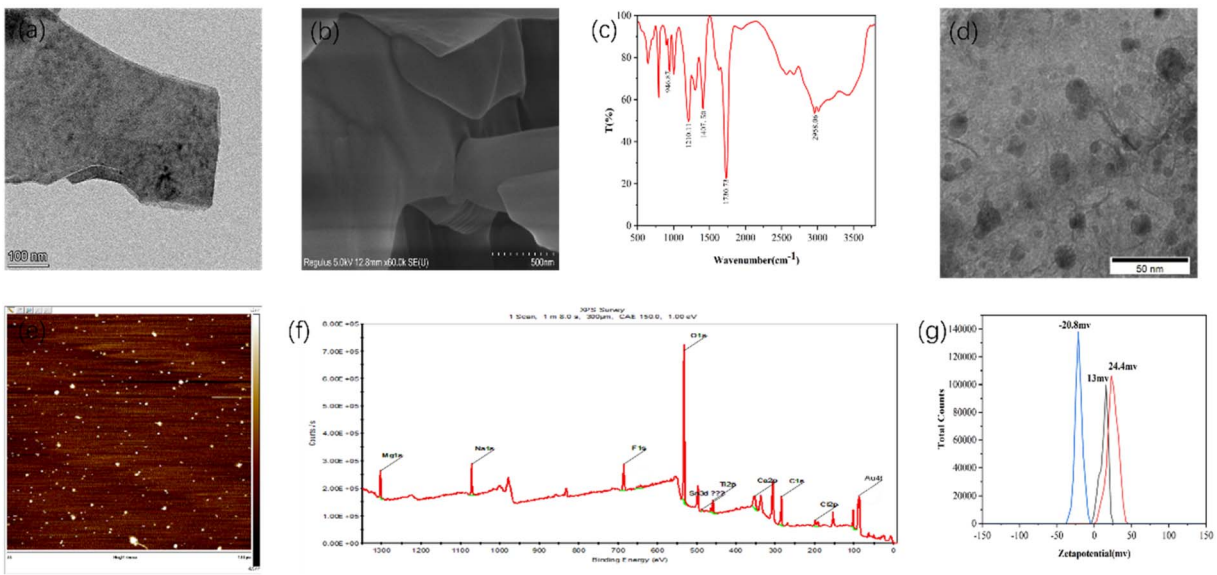

Fig. 2 (a) TEM image of Ti_2N. (b) SEM image of Ti_2N. (c) Infrared spectroscopy of Ti_2N–COOH. (d) TEM image of Au–Ti_2N–COOH. (e) AFM of Au–Ti_2N–COOH. (f) XPS survey spectrum of Au–Ti_2N–COOH. (g) Zeta-potential of Ti_2N, Ti_2N–COOH and Au–Ti_2N–COOH.

characterizations, it can be seen that the Al element has been etched away. Fig. (S6)† represents the XPS characterization of the Ti_2N–COOH material, further confirming the absence of Au elements. Fig. 2(f) shows the XPS characterization of the Au–Ti_2N–COOH material, where the absorption peaks at 532 eV, 284 eV, and 88 eV correspond to O 1s, C 1s, and Au 4f, respectively.

Fig. 2(g) presents three zeta potential graphs representing the zeta potentials of the Ti_2N material, Ti_2N–COOH material, and Au–Ti_2N–COOH material, which are measured to be 13 mV, 24.4 mV, and −20.8 mV, respectively. These measurements further confirm the successful carboxyl group modification in the second step and the successful gold particle decoration in the third step.

3.3. Experimental conditions optimization

The SERS signals of melamine powder, 4-MBA powder, and mixture of melamine and 4-MBA were first measured. As shown in Fig. S8–S10,† the characteristic peak of melamine powder is located at 707 cm^{-1} and 4-MBA is located at 1560 cm^{-1}.

To enhance the sensitivity of the substrate, various experimental conditions were optimized using melamine as the target analyte. A fixed concentration of 4-MBA was dropped separately onto glass, paper, and silicon substrates. After drying, the SERS signals were detected. Fig. 3(a–c) shows the Raman spectra of 4-MBA recorded on glass substrates, paper substrates, and silicon substrates at different concentrations. From the images, it can be observed that the background peak signals are more robust on paper substrates and glass substrates. In contrast, the background peak on the silicon substrate is located at 520 cm^{-1}, which does not interfere with the target peak region we are interested in. Therefore, in the subsequent experiments, silicon wafers were used as substrates to minimize the impact of errors on the investigation.

Firstly, the SERS signals of the Ti_2N–COOH material and the Au–Ti_2N–COOH material modified with gold nanoparticles were measured. Fig. S11† shows that the Ti_2N–COOH and Au–Ti_2N–COOH materials do not have obvious SERS characteristic peaks, and the SERS signals do not interfere with the signals of the targets. Subsequently, the impact of different modifications on sensitivity was investigated when decorating various substances on MXene materials. Equal concentrations of melamine were dropped into the substrate solutions containing the same volume and concentration. After thorough mixing, 10 μL of the mixture was dropped onto silicon wafer substrates and dried for detection. The characteristic peak of melamine is around 707 cm^{-1} and is due to the respiratory vibration of the triazine ring. In Fig. 4(a), a comparison revealed that when detecting the same concentration of melamine using pure MXene material and carboxyl-functionalized MXene material, no characteristic peak was observed. However, when using gold nanoparticles modified MXene material and MXene material simultaneously modified with carboxyl functional groups and gold nanoparticles, characteristic peaks of the target substance were detected, and the MXene material simultaneously modified with carboxyl functional groups and gold nanoparticles exhibited slightly higher peak intensity. This experimentation confirms that different substrate modifications result in varying degrees of changes in the target substance's enrichment capability and Raman signal amplification. To enhance the substrate's enrichment capability for the target substance and achieve more significant Raman signal enhancement, subsequent experiments used MXene material simultaneously modified with carboxyl functional groups and gold nanoparticles as the substrate.

Next, the optimization of material concentration was carried out by diluting the substrate solution to concentrations ranging from 10 to 60 mg kg^{-1}. The same volume of melamine at an equal concentration was then added to each diluted substrate solution. After thorough mixing,10 μL of the mixture of the substrate and target analyte was dropped onto silicon wafer substrates and dried for detection. Fig. 4(b) reveals that the SERS signal peak is highest when the substrate solution concentration is set at 40 mg kg^{-1}. This experimentation underscores that different concentrations of substrate materials impact the Raman signal. When the concentration is too low, the Raman signal does not increase to the optimal level. Conversely, excessive concentration might weaken the material's amplification capability. Therefore, in the subsequent experiments, a substrate solution concentration of 40 mg kg^{-1} was used consistently.

Moving forward, the difference in SERS signals between 4-MBA modified and unmodified 4-MBA was compared. Equal concentrations of melamine were separately added to substrate solutions containing the same volume and concentration of 4-MBA, one being modified and the other unmodified. After thorough mixing, 10 μL of the mixture of the substrate and

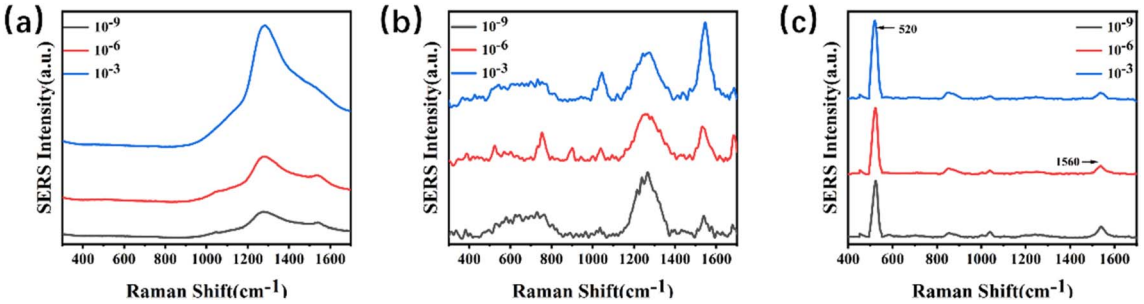

Fig. 3 (a–c) Stack plots of Raman spectra for various concentrations of 4-MBA on a SERS substrate. (a) Glass; (b) paper; (c) silicon.

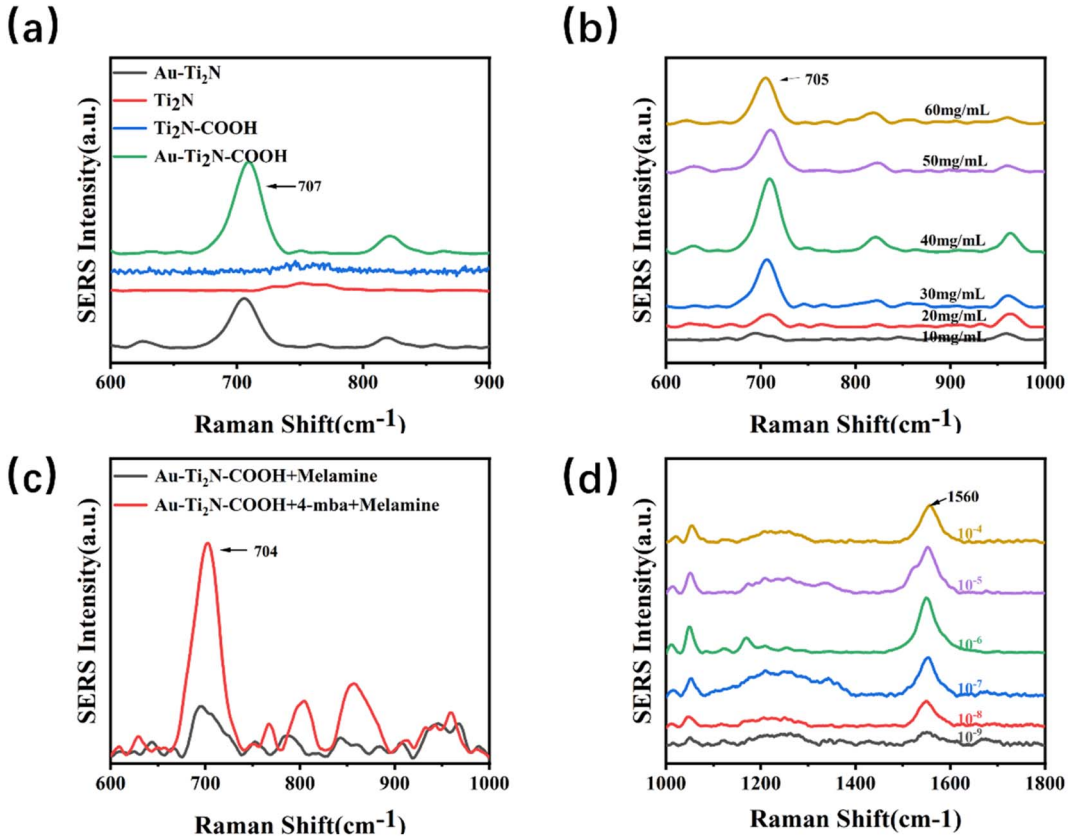

Fig. 4 (a) SERS characteristic peaks at 707 cm^{-1} for four different substrates (b) the SERS characteristic peak at 707 cm in substrate detection exhibits different intensities at various concentrations. (c) The relationship between Raman intensity and 4-MBA. (d) The relationship between different concentrations of 4-MBA and SERS characteristic peak values.

target analyte was taken and dropped onto silicon wafer substrates, followed by drying for detection. Fig. 4(c) shows that the Raman signal from the substrate modified with 4-MBA is significantly stronger than that from the unmodified 4-MBA substrate. Due to the enriching effect of the carboxyl functional group on the target analyte, increasing the concentration of carboxyl functional groups on the substrate surface enhances the substrate's enrichment capability for the target analyte, thus detecting a stronger Raman signal.

Concentrations ranging from 1×10^{-4} to 1×10^{-9} M of 4-MBA solution were separately added to substrate solutions containing the same concentration. After a half-hour reaction, equal concentrations of melamine were added to the substrate solutions, followed by thorough mixing 10 μL of the mixture of the substrate material and target analyte was taken and dropped onto silicon wafer substrates, then dried for detection. Fig. 4(d) shows that the characteristic peaks around 1560 cm^{-1} are due to the C–C expansion vibration on the benzene ring, and the characteristic peaks around 1060 cm^{-1} are due to the C–H expansion vibration on the benzene ring. The characteristic peak is most pronounced around 1560 cm^{-1}, so this peak is mainly observed to judge the difference in the enhancement effect caused by the concentration. It shows that as the concentration of 4-MBA increases, the peak of the Raman signal gradually increases. When the concentration is 1×10^{-6} M, the Raman signal is significantly the strongest. As the concentration continues to increase, the Raman signal weakens. To achieve optimal signal enhancement, subsequent experiments used a 1×10^{-6} M 4-MBA solution to modify the substrate.

The enhancement factor (EF) was determined according to the formula below.[34]

$$EF = (I_{SERS}/C_{SERS})/(I_{ref}/C_{ref})$$

where I_{SERS} and C_{SERS} denote SERS spectrum intensity and the concentration of 4-MBA molecules adsorbed on the Au–Ti_2N–COOH thin film substrate, respectively. I_{ref} and C_{ref} denote the non-SERS spectrum intensity and the concentration of 4-MBA molecules adsorbed on silicon substrate, respectively. The Raman peak intensity at 1570 cm^{-1} was used to estimate EF. The reference concentration of 4-MBA molecules was determined to be 10^{-8} M for C_{SERS} and 10^{-2} M for C_{ref}. The EF was derived to 1.63×10^6 for the Au–Ti_2N–COOH thin film substrate. Compared with the previous TiN as the SERS substrate, we have a higher magnitude of the enhancement factor and stronger signal amplification ability.

Also using 4-MBA as a signaling molecular probe, the SERS signal results were measured by Ti_2N–COOH material, and the results are shown in Fig. S12.†The Raman peak intensity at 1570 cm^{-1} was used to estimate EF. The reference

concentration of 4-MBA molecules was determined to be 10^{-6} M for C_{SERS} and 10^{-2} M for C_{ref}. The EF was derived to 1.27×10^4 for the Au–Ti_2N–COOH thin film substrate. Compared with the EF of Au–Ti_2N–COOH material, it was found that modifying gold nanoparticles on their surface could significantly improve the SERS signal amplification ability of the material.

3.4. Specificity, reproducibility, stability

Fig. 5(a) illustrates the Raman spectrum of the Au–Ti_2N–COOH substrate and the corresponding SERS signals of melamine and its analogues. Firstly, the Raman characteristic peaks of the substrate material were detected, and it was found that there were no obvious characteristic peaks in the target characteristic peak area After subtracting the background baseline, a characteristic peak was observed at 707 ± 5 cm^{-1},[33] which corresponds to the intense breathing vibration of the triazine ring of melamine and its analogues. This finding is significant because conventional detection is typically based on the characteristic peak at 707 cm^{-1}. At the same time as the detection of melamine, melamine monoamide, melamine diamide, dicyandiamide and cypromazine were also detected, and because the detected substances had similar structures to melamine, there were obvious characteristic peaks near 707 cm^{-1}. In the follow-up work, the ability of the substrate to detect multiple targets at the same time will be studied, and the potential of the substrate in the field of SERS will be developed. By comparison, it was found that the SERS signal intensity for the detection of melamine was significantly stronger than that of other analogues, and the enrichment ability for melamine could be improved due to the modification of carboxyl functional groups on the surface of the material, so that the SERS signal for the detection of melamine was stronger.

To determine the quantitative detection capability of the substrate and exclude the possibility of experimental variability, it was necessary to test the reproducibility of SERS spectra from samples with the same concentration but different batches. Five samples with a concentration of 100 μg kg^{-1} were prepared for SERS measurements. We test five different locations on a sample, as shown in Fig. 5(b), the SERS intensities are calculated, resulting in a relative standard deviation (RSD) of 2.38%. Although the signal intensity fluctuates at 707 cm^{-1}, the characteristic peak of the target can still be stably detected at 707 cm^{-1}.Therefore, the substrate demonstrates good quantitative capability for melamine detection.

The investigation of the stability testing ability of the substrate aimed to examine the regularity of changes over time in the environment. Three sets of parallel samples were prepared to directly detect the samples with the same concentration of 30 μg kg^{-1}. After detection, they were stored at 4 °C. Subsequent detections were performed at intervals of 1 week, 2 weeks, 3 weeks, 4 weeks, 6 weeks, and 8 weeks respectively. The changes in the peak intensity at 707 cm^{-1} are observed, as

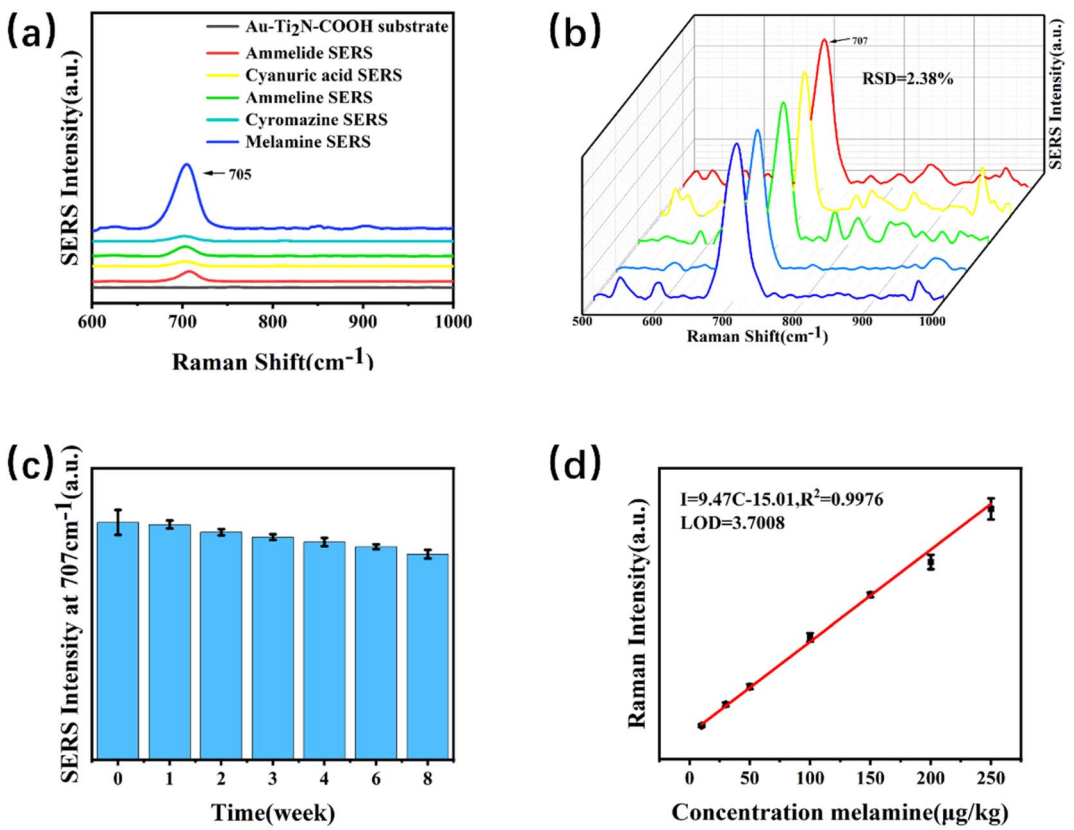

Fig. 5 (a) SERS characteristic peaks of different target substances. (b) SERS spectra of melamine (100 μg kg^{-1}) were measured from 5 samples. (c) SERS characteristic peaks of melamine at other time points. (d) Calibration curve of melamine in milk.

shown in Fig. 5(c). The peak intensity was highest when directly detected. Only the initial 98.11% in the first week after the first week, a significant decrease in the peak intensity of the samples was observed. The second week was only 95.91% compared to the initial the peak intensity in the second week was slightly lower compared to the results of the first week. The peak intensity in the third week showed little change compared to the second week. Compared with the initial 93.77% in the third week, the SERS signal intensity after the third week decreased slightly with time, and the change was not obvious. Week 8 was 86.59% relative to the initial. Therefore, the SERS signal of the substrate exhibited an overall decreasing trend over time, but the decrease was not significant. Subsequently, the SERS signal reached a stable state.

3.5. SERS measurement of melamine in liquid milk

SERS testing was conducted on samples of melamine with different concentrations. A linear model for determining the melamine content within the range of 10–250 μg kg^{-1} was obtained, as shown in Fig. 5(d). Within the linear range, the equation for the relationship between intensity (I) and concentration (C) was $I = 9.47\ C = 15.01$, $R^2 = 0.9976$, with an R-squared value of 0.9976. By measuring the signal-to-noise ratio and the slope of the linear fit equation, the limit of detection (LOD) was calculated to be 3.7008 μg kg^{-1}.

3.6. Recovery rate experiment and anti-interference experiment

The reliability and accuracy of the method were further validated through spiking and recovery experiments using actual milk samples. As shown in Table 1, SERS testing is performed on melamine samples with concentrations of 50 μg kg^{-1}, 200 μg kg^{-1}, and 250 μg kg^{-1}. Based on the predicted concentrations obtained from the fitting equation, the recovery rates of this method range from 99.84% to 107.55%, with a relative standard deviation (RSD) of approximately 5%.

3.7. Comparison of reported analytical methods

Table 2 compiles the comparison of the analytical features of the selected references. Compared to the reported methods, similar detection levels for the analysis of melamine were obtained in this study. These methods have long detection times and complex preprocessing processes, requiring specialized operators. Such as extraction and cleanup of melamine in milk samples. The SERS technique used in this study is simple to operate, with an integration time of only 10 seconds, which is much less than the time required by other methods. Therefore, the proposed method provided a relatively sensitivity and rapid analysis of melamine in milk samples.

Table 1 Predicted results of melamine in milk ($n = 3$)

Spiked (μg kg^{-1})	Detected (μg kg^{-1})	Recovery (%)	Relative standard deviation (%)
50	53.7732	107.55	5.22
200	199.6837	99.84	5.53
250	268.3860	107.35	3.24

Table 2 Comparison of various analytical methods developed for analysis of melamine in several matrixes

Matrix	Analysis	LOD (μg kg^{-1})	Ref.
Milk and milk powder	HPLC-HRMS	0.6	35
Milk	NIR	1.2	36
Milk	ELISA	0.3	16
Milk	Fluorescence	68	37
Milk	SERS	3.7	This work

4. Conclusion

In this study, we introduced Au–Ti_2N–COOH material as a novel SERS substrate for melamine detection. This method demonstrates exceptional sensitivity and accuracy, eliminating the necessity for complex sample pretreatment. The detection limit in liquid milk stands at 3.7008 μg kg^{-1}, with spike recovery rates ranging from 99.84% to 107.55% and an approximate RSD of 5%. The results of the recovery experiments further corroborate the method's reliability. In conclusion, this new SERS substrate holds significant potential for applications in food safety applications.

Conflicts of interest

There are no conflicts to declare.

Acknowledgements

This work was supported by the National Key Research and Development Program of China (Grant No. 2021YFA0910200).

References

1 A. K. Hau, T. H. Kwan and P. K. Li, Melamine toxicity and the kidney, *J. Am. Soc. Nephrol.*, 2009, **20**(2), 245–250.
2 G. Xiao, L. Li, A. Yan and X. He, Direct detection of melamine in infant formula milk powder solution based on SERS effect of silver film over nanospheres, *Spectrochim. Acta, Part A*, 2019, **223**, 117269.
3 J. L. Dorne, D. R. Doerge, M. Vandenbroeck, J. Fink-Gremmels, W. Mennes, H. K. Knutsen, F. Vernazza, L. Castle, L. Edler and D. Benford, Recent advances in the risk assessment of melamine and cyanuric acid in animal feed, *Toxicol. Appl. Pharmacol.*, 2013, **270**(3), 218–229.
4 P. Ma, F. Liang, Y. Sun, Y. Jin, Y. Chen, X. Wang, H. Zhang, D. Gao and D. Song, Rapid determination of melamine in milk and milk powder by surface-enhanced Raman spectroscopy and using cyclodextrin-decorated silver nanoparticles, *Microchim. Acta*, 2013, **180**(11), 1173–1180.
5 J. W. DeVries, G. W. Greene, A. Payne, S. Zbylut, P. F. Scholl, P. Wehling, J. M. Evers and J. C. Moore, Non-protein nitrogen

determination: A screening tool for nitrogenous compound adulteration of milk powder, *Int. Dairy J.*, 2017, **68**, 46–51.

6 A. Sarafraz Yazdi, S. Raouf Yazdinezhad and T. Heidari, Determination of melamine in soil samples using surfactant-enhanced hollow fiber liquid phase microextraction followed by HPLC-UV using experimental design, *J. Adv. Res.*, 2015, **6**(6), 957–966.

7 A. Fashi, M. R. Yaftian and A. Zamani, Determination of melamine in dairy products using electromembrane-LPME followed by HPLC, *Food Chem.*, 2015, **188**, 92–98.

8 C. F. Nascimento, P. M. Santos, E. R. Pereira-Filho and F. R. P. Rocha, Recent advances on determination of milk adulterants, *Food Chem.*, 2017, **221**, 1232–1244.

9 M. Ezhilan, M. B. Gumpu, B. L. Ramachandra, N. Nesakumar, K. J. Babu, U. M. Krishnan and J. B. B. Rayappan, Design and development of electrochemical biosensor for the simultaneous detection of melamine and urea in adulterated milk samples, *Sens. Actuators, B*, 2017, **238**, 1283–1292.

10 S. Wu, Z. Z. Yin, X. Chen, X. Wang, D. Wu and Y. Kong, Electropolymerized melamine for simultaneous determination of nitrite and tartrazine, *Food Chem.*, 2020, **333**, 127532.

11 Z. Wang, X. Ma, L. Zhang, W. Yang, L. Gong, P. He and Z. Li, Screening and determination of melamine residues in tissue and body fluid samples, *Anal. Chim. Acta*, 2010, **662**(1), 69–75.

12 X. Zhu, S. Wang, Q. Liu, Q. Xu, S. Xu and H. Chen, Determination of residues of cyromazine and its metabolite, melamine, in animal-derived food by gas chromatography-mass spectrometry with derivatization, *J. Agric. Food Chem.*, 2009, **57**(23), 11075–11080.

13 H. Kuang, W. Chen, W. Yan, L. Xu, Y. Zhu, L. Liu, H. Chu, C. Peng, L. Wang, N. A. Kotov and C. Xu, Crown ether assembly of gold nanoparticles: Melamine sensor, *Biosens. Bioelectron.*, 2011, **26**(5), 2032–2037.

14 Z. Wu, H. Zhao, Y. Xue, Q. Cao, J. Yang, Y. He, X. Li and Z. Yuan, Colorimetric detection of melamine during the formation of gold nanoparticles, *Biosens. Bioelectron.*, 2011, **26**(5), 2574–2578.

15 Y. Zhou, C.-Y. Li, Y.-S. Li, H.-L. Ren, S.-Y. Lu, X.-L. Tian, Y.-M. Hao, Y.-Y. Zhang, Q.-F. Shen, Z.-S. Liu, X.-M. Meng and J.-H. Zhang, Monoclonal antibody based inhibition ELISA as a new tool for the analysis of melamine in milk and pet food samples, *Food Chem.*, 2012, **135**(4), 2681–2686.

16 J.-W. Choi, K.-M. Min, S. Hengoju, G.-J. Kim, S.-I. Chang, A. J. deMello, J. Choo and H. Y. Kim, A droplet-based microfluidic immunosensor for high efficiency melamine analysis, *Biosens. Bioelectron.*, 2016, **80**, 182–186.

17 N. Vasimalai and S. Abraham John, Picomolar melamine enhanced the fluorescence of gold nanoparticles: spectrofluorimetric determination of melamine in milk and infant formulas using functionalized triazole capped gold nanoparticles, *Biosens. Bioelectron.*, 2013, **42**, 267–272.

18 D. Huang, J. Zhao, M. Wang and S. Zhu, Snowflake-like gold nanoparticles as SERS substrates for the sensitive detection of organophosphorus pesticide residues, *Food Control*, 2020, **108**, 106835.

19 B. X. Wang, G. Duan, W. Xu, C. Xu, J. Jiang, Z. Yang, Y. Wu and F. Pi, Flexible surface-enhanced Raman scatting substrates: recent advances in their principles, design strategies, diversified material selections and applications, *Crit. Rev. Food Sci. Nutr.*, 2022, 1–45.

20 C. Zong, M. Xu, L. J. Xu, T. Wei, X. Ma, X. S. Zheng, R. Hu and B. Ren, Surface-Enhanced Raman Spectroscopy for Bioanalysis: Reliability and Challenges, *Chem. Rev.*, 2018, **118**(10), 4946–4980.

21 H. L. Wang, E. M. You, R. Panneerselvam, S. Y. Ding and Z. Q. Tian, Advances of surface-enhanced Raman and IR spectroscopies: from nano/microstructures to macro-optical design, Light, *Sci. Appl.*, 2021, **10**(1), 161.

22 X. M. Qian and S. M. Nie, Single-molecule and single-nanoparticle SERS: from fundamental mechanisms to biomedical applications, *Chem. Soc. Rev.*, 2008, **37**(5), 912–920.

23 P. Karthick Kannan, P. Shankar, C. Blackman and C. H. Chung, Recent Advances in 2D Inorganic Nanomaterials for SERS Sensing, *Adv. Mater.*, 2019, **31**(34), e1803432.

24 M. Naguib, M. Kurtoglu, V. Presser, J. Lu, J. Niu, M. Heon, L. Hultman, Y. Gogotsi and M. W. Barsoum, Two-dimensional nanocrystals produced by exfoliation of Ti_3AlC_2, *Adv. Mater.*, 2011, **23**(37), 4248–4253.

25 B. Soundiraraju and B. K. George, Two-Dimensional Titanium Nitride (Ti_2N) MXene: Synthesis, Characterization, and Potential Application as Surface-Enhanced Raman Scattering Substrate, *ACS Nano*, 2017, **11**(9), 8892–8900.

26 P. K. Kalambate, N. S. Gadhari, X. Li, Z. Rao, S. T. Navale, Y. Shen, V. R. Patil and Y. Huang, Recent advances in MXene–based electrochemical sensors and biosensors, *TrAC, Trends Anal. Chem.*, 2019, **120**, 115643.

27 Z. He, T. Rong, Y. Li, J. Ma, Q. Li, F. Wu, Y. Wang and F. Wang, Two-Dimensional TiVC Solid-Solution MXene as Surface-Enhanced Raman Scattering Substrate, *ACS Nano*, 2022, **16**(3), 4072–4083.

28 D. Liu, W. Yi, Y. Fu, Q. Kong and G. Xi, In Situ Surface Restraint-Induced Synthesis of Transition-Metal Nitride Ultrathin Nanocrystals as Ultrasensitive SERS Substrate with Ultrahigh Durability, *ACS Nano*, 2022, **16**(8), 13123–13133.

29 A. Sarycheva, T. Makaryan, K. Maleski, E. Satheeshkumar, A. Melikyan, H. Minassian, M. Yoshimura and Y. Gogotsi, Two-Dimensional Titanium Carbide (MXene) as Surface-Enhanced Raman Scattering Substrate, *J. Phys. Chem. C*, 2017, **121**(36), 19983–19988.

30 Y. Peng, C. Lin, L. Long, T. Masaki, M. Tang, L. Yang, J. Liu, Z. Huang, Z. Li, X. Luo, J. R. Lombardi and Y. Yang, Charge-Transfer Resonance and Electromagnetic Enhancement Synergistically Enabling MXenes with Excellent SERS Sensitivity for SARS-CoV-2 S Protein Detection, *Nano–Micro Lett.*, 2021, **13**, 52.

31 L. Lan, X. Fan, S. Yu, J. Gao, C. Zhao, Q. Hao and T. Qiu, Flexible Two-Dimensional Vanadium Carbide MXene-Based Membranes with Ultra-Rapid Molecular Enrichment for Surface-Enhanced Raman Scattering, *ACS Appl. Mater. Interfaces*, 2022, **14**(35), 40427–40436.

32 S. K. Bhardwaj, H. Singh, M. Khatri, K. H. Kim and N. Bhardwaj, Advances in MXenes-based optical biosensors: A review, *Biosens. Bioelectron.*, 2022, **202**, 113995.

33 M. Y. Li, Q. Liao, M. Zhang, X. C. Ai and F. Y. Li, Surface-enhanced Raman scattering and DFT computational studies of a benzotriazole derivative, *J. Mol. Struct.*, 2008, **888**(1), 2–6.

34 H. Wei, M. Wu, Z. Dong, Y. Chen, J. Bu, J. Lin, Y. Yu, Y. Wei, Y. Cui and R. Wang, Composition, microstructure and SERS properties of titanium nitride thin film prepared *via* nitridation of sol–gel derived titania thin films, *Raman Spectrosc.*, 2017, **48**, 578–585.

35 D. Chen, Y. Zhao, H. Miao and Y. Wu, A novel dispersive micro solid phase extraction using PCX as the sorbent for the determination of melamine and cyromazine in milk and milk powder by UHPLC-HRMS/MS, *Talanta*, 2015, **134**, 144–152.

36 J. Lim, G. Kim, C. Mo, M. S. Kim, K. Chao, J. Qin, X. Fu, I. Baek and B. K. Cho, Detection of melamine in milk powders using near-infrared hyperspectral imaging combined with regression coefficient of partial least square regression model, *Talanta*, 2016, **151**, 183–191.

37 M. C. Barreto, R. G. Braga, S. G. Lemos and W. D. Fragoso, Determination of melamine in milk by fluorescence spectroscopy and second-order calibration, *Food Chem.*, 2021, **364**, 130407.